

# Biologically Plausible Deep Learning

Yali Amit

University of Chicago

October 11, 2024

## Abstract

Building on the model proposed in [7] we show that deep networks can be trained using biologically plausible Hebbian rules yielding similar performance to ordinary back-propagation. To overcome the unrealistic symmetry in connections between layers, implicit in back-propagation, the feedback weights are separate from the feedforward weights. But, in contrast to [7], they are also updated with a local rule - a weight is updated solely based on the activity of the units it connects. With fixed feedback weights the performance degrades quickly as the depth of the network increases, when they are updated the performance is comparable to regular back-propagation. We also propose a cost function whose derivative can be represented as a local update rule on the last layer. Convolutional layers are updated with tied weights across space, which is not biologically plausible. We show that similar performance is achieved with sparse layers corresponding to the connectivity implied by the convolutional layers, but where weights are untied and updated separately. In the linear case we show theoretically that the convergence of the error to zero is accelerated by the update of the feedback weights.

## 1 Introduction

The success of deep networks in a range of prediction tasks has raised the question of whether they can serve as models for processing in the cortex [4, 8]. These networks are most successful when trained using versions of stochastic gradient descent, where small random subsets of training data are used to compute the gradient of the loss function with respect to the weights connecting subsequent layers and then update them. Due to the particular structure of the function represented by these multi-layer networks the

gradient is computed using back-propagation - an algorithmic formulation of the chain rule. In all but the last layer, the gradient of a weight in this algorithm is a product of the activity of the units it connects - the pre-synaptic input unit in the lower layer and the post-synaptic output unit in the higher layer. In that sense it is performing a form of local Hebbian learning: the update depends on the product of the feedback activity in the post-synaptic unit (the error signal) and the activity of the pre-synaptic unit. However a fundamental element of back-propagation is not biologically plausible as summarized very succinctly in [7]. Prior to a weight update, the error signal of the post-synaptic unit is computed as a function of units in layers above it in the hierarchy in terms of the *same* weight matrix used to compute the feedforward signal, implying a symmetric synaptic connectivity matrix. This is an unrealistic assumption, although reciprocal physical connections between neurons are more common than would be expected at random, these connections are physically separated in entirely different regions of the neuron and can in no way be the same. Furthermore, with the most commonly used final layer - the softmax - gradient computation is a function of the entire connectivity matrix feeding into that layer, which violates the local update rule. Finally, although convolutional layers are consistent with the structure of retinotopic layers in visual cortex, backpropagation through these layers is not biologically plausible. Since the weights of the filters applied across space are assumed identical, the gradient of the unique filter is computed as the sum of the gradients at each location. In the brain the connections corresponding to different spatial locations are physically different and one can't expect them to undergo coordinated updates.

We first show that the softmax can be avoided using a suitable multi-class loss function that is a weighted sum of perceptron type loss functions (also known as hinge functions), which we denote the *hinge* loss. This yields gradients that are computed locally - perceptron type learning rules of the type used in [1, 5, 2]. The performance is comparable to that of the softmax with cross-entropy. The idea to use a separate matrix for the feedback projections comes from [7] where it is set as a fixed random matrix that is not updated. We call this fixed random feedback - FRFB. Although in some experiments this yields reasonable results, for most network architectures the results are far inferior to those using regular back propagation. One remedy proposed in [6] is to introduce layer-wise normalization of the outputs. This yields results with random feedbacks that are close to momentum based gradient descent of the back-propagation algorithm for certain network architectures. However the propagation of the gradient through the normalization layer is complex and it

is unclear how to implement it in a network. Furthermore [6] shows that a simple transfer of information on the sign of the actual back-propagation gradient yields an improvement on using the purely random back-propagation matrix. It is however unclear how such information could be transmitted between different synapses. Also in their experiments they used the softmax classification cost function, and the layerwise batch normalization introduces gradients and error propagations that are difficult to implement biologically.

In our experiments we also maintain a strict separation of the back propagation matrix and the feedforward matrix, both are randomly initialized, but we add a local Hebbian update on each feedback connection. We call this updated random feedback - URFB. The update is again the product of the error signal in the post-synaptic unit and the input of the pre-synaptic unit. Thus if two units are connected in both directions the feedback update is the same as the feedforward update. But, since the connections between two units (if they both exist) are initialized separately they do not end up with the same value. A similar update idea is proposed in [9], but in the analysis of their algorithm, they assume that in the long run, since the updates are the same the synaptic values are the same, which is definitely not the case. We also experiment with randomly zeroing out half of the connections, separately for feedforward and feedback connections. Thus not only are the matrices different, but connectivity is asymmetric.

Finally, we replace the commonly used unbounded rectified linear unit, with a saturated linearity  $\sigma(x) = \min(\max(x, -1), 1)$ , which is more biologically plausible, we avoid normalization layers whose gradient is quite complex and not easily amenable to neural computation, and we run all experiments with the simplest stochastic gradient descent that does not require any memory of earlier gradients.

We find that as the networks grow deeper, the performance of the fixed random matrix feedback (FRFB) deteriorates while the performance of the URFB is quite close to that of the benchmark stochastic gradient descent with back-propagation. It is important to perform these experiments with convolutional layers because typically, in image classification, depth yields improvements in classification rates only when convolutions and pooling are introduced. Using multiple fully connected layers rarely makes any difference.

This leads us to the final set of experiments where instead of purely convolutional layers we use a connectivity matrix that has the sparsity structure inherited from the convolution but the values in the matrix are ‘untied’ undergo independent local updates. The memory requirements of such layers are much greater than for convolutional layers, as is the computation, so for these experiments we restrict to simpler architectures. Overall

we observe the same phenomena as with convolutional layers, namely the update of the feedback connections yields performance close to that of regular backpropagation.

In section 2.1 we provide the details of the classification loss function and propose a local network of three neurons to implement the derivative of the loss, in section 2.2 we explain the updated random feedback rule. In section 3 we provide a theoretical analysis of the linear version of this form of update and show that updating the feedback connections yields faster convergence than fixed feedback connections. In section 4 we report a number of experiments and illustrate some interesting properties of these networks. We end with a discussion on the remaining aspects of the proposed architecture that are still not biologically plausible and discuss possible solutions.

## 2 The updated random feedback algorithm

The softmax loss commonly used in deep learning does not lend itself to Hebbian updates as the error signal involves a normalization with respect to the activity of all output units, and the derivative involves non-local computations. Other hinge based multi-class losses involve the maximum of all outputs other than the correct class and their derivative also involves non-local computation. In this section we describe a loss function, whose derivatives can be computed locally, yielding a Hebbian field dependent update of the weights connecting to the final output layer. Then we describe the modified back-propagation of the error signal through the layers of the network using separate feedback connections. Back-propagation of the error signal is computed as a simple linear combination of error signals in the layer above, starting with the error signal at the output layer. This output error is the derivative of the loss with respect to the input field to each output unit. It is a complex function of the input field and needs to be represented in the activity of the output unit in order for back-propagation to occur. In section 2.3 we propose a simple network to compute this function in the output layer.

### 2.1 Loss function

The classification loss function used here is based on the hinge loss used in standard linear SVMs. In the two class problem with classes labeled  $\pm 1$  it is defined as:

$$\mathcal{C}(w) = [1 - y\langle w, x \rangle]_+ = 1_{y=1}[1 - \langle w, x \rangle]_+ + 1_{y=-1}[1 + \langle w, x \rangle]_+. \quad (1)$$

The derivative of this loss with respect to  $w_i$ , for a single example  $x, y$  yields the perceptron learning rule *with margin*:

$$\Delta w_i = \begin{cases} x_i & \text{if } y = 1 \text{ and } \langle w, x \rangle \leq 1 \\ -x_i & \text{if } y = -1 \text{ and } \langle w, x \rangle \geq -1, \\ 0 & \text{otherwise} \end{cases} \quad (2)$$

(adding a shrinkage update  $w_i^{new} = w_i^{old} - \eta(\Delta w_i + \lambda w_i)$ , yields a stochastic gradient descent algorithm for SVM's with a squared norm penalty), see [11]. If we think of the supervised signal as activating a unit  $y$  with +1 for one class -1 for the other the update rule can be rewritten as  $\Delta w_i = y \cdot x_i$  if the input field  $h = \langle w, x \rangle$  satisfies  $\text{sign}(y)h \leq 1$ . This update rule is Hebbian in that it is locally computed from the activity of the pre and post synaptic units  $x_i, y$ , except for the dependence on  $h$ . One might ask why not use the unconstrained Hebbian update  $\Delta w_i = y \cdot x_i$ , which corresponds to a loss that computes the inner product of  $y$  and  $x$ . Mathematically the constrained hinge loss corresponds to maximizing the margin between the two classes. Intuitively, unconstrained maximization of the inner product can yield over fitting in the presence of particularly large values of some of the coordinates of  $x$  and create an imbalance between the two classes if their input feature distribution is very different. This becomes all the more important with multiple classes, which we discuss next.

For multiple classes the hinge loss can be generalized as follows. Assume  $C$  output units  $o_1, \dots, o_C$ . For an example  $x, y$ , with  $y \in \{1, \dots, C\}$  define the cost

$$\mathcal{C}(w) = [1 - \langle W_y, x \rangle]_+ + \mu \sum_{c \neq y} [1 + \langle W_c, x \rangle]_+, \quad (3)$$

where  $W_c$  are the weights feeding into output unit  $o_c$ , and  $\mu$  is some balancing factor. If on presentation of an example from class  $c$  we set unit  $o_c$  to 1 and all the others to  $-\mu$  the update rule for this classification cost is again Hebbian, with a field constraint. For weight  $W_{ic}$  connecting a unit  $x_i$  from the input layer to a unit  $o_c$  in the output layer

$$-\frac{\partial \mathcal{C}}{\partial W_{ic}} = \begin{cases} x_i & \text{if } o_c = 1 \text{ and } \langle W_c, x \rangle < 1 \\ -\mu x_i & \text{if } o_c = -\mu \text{ and } \langle W_c, x \rangle > -1 \\ 0 & \text{otherwise,} \end{cases} \quad (4)$$

i.e.  $\Delta W_{ic} = o_c x_i$  if  $\text{sign}(o_c)h_c \leq 1$ , where  $h_c = \langle W_c, x \rangle$ . All experiments below use this rule. To anticipate the notation for backpropagation we write  $\delta_c = \frac{\partial \mathcal{C}}{\partial h_c}$  - the error at unit  $c$ . We have

$$\delta_c = \begin{cases} 1 & \text{if } o_c = 1 \text{ and } h_c \leq 1 \\ -\mu & \text{if } o_c = -\mu \text{ and } h_c \geq 1 \\ 0 & \text{otherwise.} \end{cases} \quad (5)$$

In effect this loss implements the well known one-against-the-rest method for multi-class SVM's. Each unit  $o_c$  can be viewed as a classifier of class  $c$  against all the rest. When an example of class  $c$  is presented it updates the weights to obtain a more positive output, when an example of any class other than  $c$  is presented it updates the weights to obtain a more negative output. For testing the network computes the output unit with largest activation. In [1, 2] a network of binary neurons with discrete synapses was implemented that used similar type of field based Hebbian learning rule to update connections between neurons in the input and output layers. Each class was represented by multiple neurons in the output layer. Thus classification was achieved through recurrent dynamics in the output layer, where the class with most activated units maintained sustained activity, whereas activity in the units corresponding to other classes died out.

## 2.2 Updated asymmetric feedback connections

In a multilayer net let  $x_l$  be the output of layer  $l$  with  $l = 0$  denoting the input layer and  $L$  the output layer with  $C$  units  $o_1, \dots, o_C$ . Let  $W_{l,i}$  be the feedforward weights connecting layer  $l-1$  to unit  $i$  in layer  $l$  and  $R_{l,j}$  be the feedback weights connecting layer  $l$  to unit  $j$  in layer  $l-1$ . Denote by  $h_{l,i} = \langle W_{l,i}, x_{l-1} \rangle$  the input field to layer  $l$ . Then  $x_{l,i} = \sigma(h_{l,i})$  where  $\sigma$  is a non-linearity. Back-propagation is summarized in two equations:

$$\begin{aligned} \frac{\partial \mathcal{C}}{\partial W_{l,i,j}} &= \delta_{l,i} \sigma'(h_{l,i}) x_{l-1,j} \\ \delta_{l-1,j} &= \sum_i R_{l,j,i} \delta_{l,i}, \end{aligned} \quad (6)$$

Starting with  $\delta_{Lc}$  as defined in equation (5) for the output layer this defines a backwards recursion for the update of the weights  $W_l, l = L, \dots, 1$ . Note that once  $\delta_L$  is computed, all weight updates are local and Hebbian, involving a product of the activity of the post-synaptic unit  $\delta_{l,i}$  the pre-synaptic( unit  $x_{l-1,j}$  and function  $\sigma'(h_{l,i})$  of the field of the

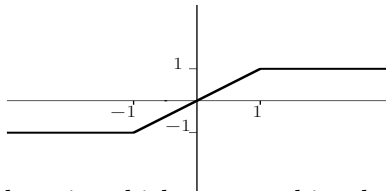
post-synaptic unit. If we set  $R_{l,ji} = W_{l,ij}$  we get the actual computation of the gradient of the loss function with respect to the weights  $W$ . However this implies a strictly symmetric connectivity in the network, which is not biologically plausible (see [7]).

In [7] the use of fixed random feedback (FRFB) connections  $R$  was introduced. This removes the symmetry and the algorithm no longer computes a gradient of a cost function. For deeper networks with more challenging data sets there is a significant loss of performance with fixed random feedback connections. In [6] batch normalization was introduced after each layer of the network and significantly improved the result of the FRFB architecture. However the back-propagation of the gradient of the batch-normalization is complex and it is not clear how it could be implemented in a network of neurons. Furthermore [6] experimented with a minimal transfer of information from the feedforward to the feedback connections in the form of their *sign*. I.e.  $R_{new} = \text{sign}(W_{new})$  or  $R_{new} = R \cdot \text{sign}(W_{new})$ , where  $R$  are the fixed random feedback connections. Combined with batch-normalization this performed somewhat better than the fixed random feedback connections.

We propose a different form of modification for the feedback connections that does not require any direct transfer of information from the feedforward connections, is also local and Hebbian, and eliminates the need for batch normalization. Simply, the connection  $R_{l,ji}$  experiences the same activity in the two units it connects as the connection  $W_{l,ij}$  and so we update it with the same increment:

$$\Delta R_{l,ji} = \Delta W_{l,ij} = \delta_{l,i} \sigma'(h_{l,i}) x_{l-1,j}. \quad (7)$$

Thus  $R_{l,ji}$  and  $W_{l,ij}$  are initialized differently but undergo the same modifications. We call this method *updated random feedback* URFB. This is also proposed in [9] but in the analysis it is assumed that these two weights end up being the same, which is never the case.



too low, in which case nothing happens. This, again, is a field dependent learning rule, which could be implemented internally to the neuron since this signal does not need to be propagated. In addition, in order to increase the plausibility of the model we also

experiment with sparsifying the feedforward and feedback connections by randomly fixing half of each set of weights at 0.

### 2.3 Local network for output error computation

The error signal of the output layer needs to be represented in the activity of the output units. The supervisory signal is simply  $o_c = 1$  or  $o_c = -\mu$  depending on whether class  $c$  is presented or a different class. However the error signal defined in equation (5) is a complicated function of this supervisory signal as it depends on the input field of the unit. In [5] the authors attempt to find a biological underpinning for the field-dependent Hebbian learning rule in terms of single cell neurobiology. A mechanism internal to the neuron is proposed, that shuts off potentiation or depression of its incoming synapses when the field is too high or too low. However, shutting off synaptic modifications, does not manifest itself in the activity of the neuron. An implementation that is internal to the neuron provides no explicit ‘error’ signal, which can be propagated to previous layers. When the network only has two layers, an input and an output, that is not an issue, but with deeper networks we will need to use feedback connections to propagate the error signal.

Here we propose a small local circuit that can implement the field dependent learning rule with the error signal manifesting itself in the activity of a particular neuron. To avoid complications of modeling excitatory and inhibitory neurons we assume neurons have positive and negative firing rates and synaptic connections are positive and negative. The main idea is to introduce a control unit  $t_c$  that shuts the main unit  $o_c$  off when the field is outside the appropriate range.

Let  $o_c$  be the firing rate of a neuron associated with class  $c$  with input field given by  $h_c = \langle W_c, x \rangle$ . Assume  $h_c$  always lies in the interval  $[-M, M]$ . Given a learning threshold  $S$  (in the previous section we had  $S = 1$ ), we want  $o_c = 1$  if class  $c$  is presented and  $h_c < S$ ,  $o_c = -\mu$  if another class is presented and  $h_c > -1$  and  $o_c = 0$  otherwise. Let  $s_c$  be the unit providing the supervisory signal: 1 if class  $c$  is being presented, -1 otherwise, and let  $t_c$  be a ‘control’ neuron. The input to  $t_c$  is simply  $o_c$  and the full input field of  $o_c$  is

$$H_c = h_c + 2Ms_c - 2Mt_c, \quad (8)$$

Also  $o_c = \sigma_o(H_c)$ ,  $t_c = \sigma_t(o_c)$ .



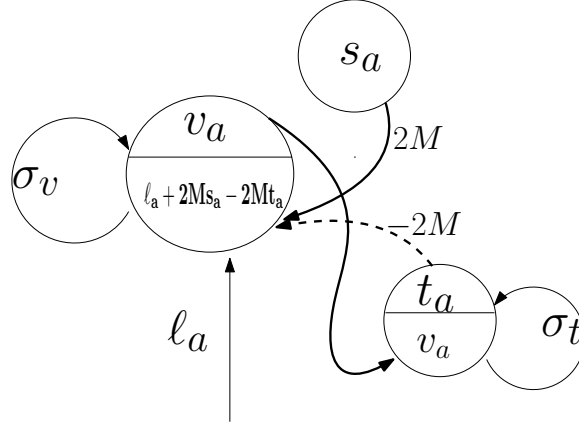


Figure 1: The circuit including the supervisory neuron  $s_a$ , the  $A$  layer neuron  $v_a$  and the control neuron  $t_a$ .

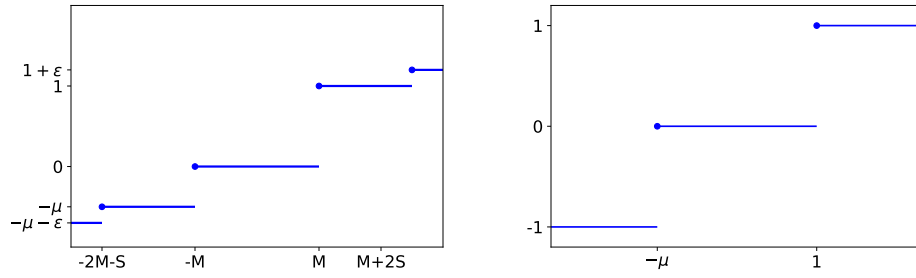


Figure 2: Left: Transfer function  $\sigma_v$ . Right: Transfer function  $\sigma_t$

Let  $\mu < 1$ . The transfer functions of  $o_c, t_c$  are given by

$$\sigma_o(x) = \begin{cases} 1 + \epsilon & \text{if } x > 2M + S \\ 1 & \text{if } x \in [M, 2M + S] \\ 0 & \text{if } x \in [-M, M] \\ -\mu & \text{if } x \in [-2M - S, -M] \\ -\mu - \epsilon & \text{if } x < -2M - S \end{cases}, \quad \sigma_t(x) = \begin{cases} 1 & \text{if } x > 1 \\ 0 & \text{if } -\mu \leq x \leq 1 \\ -1 & \text{if } x < -\mu \end{cases} \quad (9)$$

If the supervisory signal is  $s_c = 1$  and  $h_c \leq S$  then  $M \leq H_c \leq 2M + S$ , so  $o_c = 1$  and

$t_c = 0$ . This yeilds the update cycle

$$o_c = 1 \rightarrow t_c = 0 \rightarrow o_c = 1,$$

and  $o_c$  is constant at value 1.

If  $h_c > S$  then  $H_c > 2M + S$  so that  $o_c = 1 + \epsilon$  and  $t_c = 1$ . Then,  $H_c = h_c \in [-M, M]$  so that  $o_c = 0$ . This yields the update cycle:

$$o_c = 1 + \epsilon \rightarrow t_c = 1 \rightarrow o_c = 0 \rightarrow t_c = 0 \rightarrow o_c = 1 + \epsilon,$$

so that  $o_c$  oscillates between 0 and  $1 + \epsilon$ .

Conversely if the supervisory signal is  $s_c = -1$  and  $h_c \geq -S$  then  $-2M - S \leq H_c \leq -M$  so  $o_c = -\mu$  and  $t_c = 0$  yielding

$$o_c = -\mu \rightarrow t_c = 0 \rightarrow o_c = -\mu,$$

and  $o_c$  is constant at  $-\mu$ . If  $h_c < -S$  then  $H_c < -2M - S$ ,  $o_c = -\mu - \epsilon$  causing  $t_c = -1$  and  $H_c = h_c$  so that  $o_c = 0$  and we get the update cycle:

$$o_c = -\mu - \epsilon \rightarrow t_c = -1 \rightarrow v_c = 0 \rightarrow t_c = 0 \rightarrow o_c = -\mu - \epsilon,$$

so that  $o_c$  oscillates between 0 and  $-\mu - \epsilon$ .

In summary the activity of  $o_c$  is field dependent. If  $\text{sign}(o_c)h_c < S$  then  $o_c = 1, -\mu$  depending on the presented class, and  $\Delta W_{ic} = x_i o_c$ . If  $\text{sign}(o)c h_c > S$  then  $o_c$  oscillates and periodically visits the state  $o_c = 0$  and no update of synapses connecting to  $o_c$  occurs. Ignoring the oscillation this circuit can be thought of as implementing the rule in (4). The activity of  $o_c$  is precisely the signal that needs to be propagated backwards to the input layer.

### 3 Mathematical analysis of updated random feedback

The mathematical analysis closely follows the methods developed in [10] and thus focuses on linear networks, i.e.  $\sigma(x) = x$  and a simple quadratic loss. We start with a simple two layer network.

### 3.1 Two layer network

Let the input  $x \in \mathbb{R}^{n_0}$ , and the output  $y = W_2 W_1 x \in \mathbb{R}^{n_2}$  with weights  $W_1 \in \mathbb{R}^{n_1 \times n_0}$ ,  $W_2 \in \mathbb{R}^{n_2 \times n_1}$ . If  $X$  is the  $n_0 \times N$  matrix of input data and  $Y$  the  $n_2 \times N$  of output data the goal is to minimize

$$C(W_1, W_2) = \|Y - W_2 W_1 X\|^2.$$

Writing  $T = Y X^t \in \mathbb{R}^{n_2 \times n_0}$  the gradient of  $L$  with respect to  $W_1$  and  $W_2$  yield the following gradient descent ODE's:

$$\begin{aligned}\dot{W}_2 &= (T - W_2 W_1) W_1^t \\ \dot{W}_1 &= W_2^t (T - W_2 W_1),\end{aligned}\tag{10}$$

with some initial condition  $W_1(0), W_2(0)$ . If we implement the URFB described above we get the following three equations:

$$\begin{aligned}\dot{W}_2 &= (T - W_2 W_1) W_1^t \\ \dot{W}_1 &= R_2 (T - W_2 W_1) \\ \dot{R}_2 &= \epsilon W_1 (T - W_2 W_1)^t,\end{aligned}\tag{11}$$

where  $R_2 \in \mathbb{R}^{n_1 \times n_2}$  and  $\epsilon$  is a parameter. Note the  $\epsilon = 0$  corresponds to FRFB, as there is no modification of the matrix  $R$ . The URFB corresponds to  $\epsilon = 1$ . Our goal is to show that the larger  $\epsilon$  the faster the convergence of the system to a stable point.

To simplify the analysis of (11) we assume  $W_1(0) = W_2(0) = 0$  and  $R_2(0)$  is random. Then  $R_2 = R_2(0) + \epsilon W_2^t$  and the system reduces to

$$\begin{aligned}\dot{W}_2 &= (T - W_2 W_1) W_1^t \\ \dot{W}_1 &= (R_2(0) + \epsilon W_2^t) (T - W_2 W_1).\end{aligned}\tag{12}$$

Now let  $T = U \Lambda_T V^t$  be the SVD of  $T$ . Assuming  $n_2 \leq n_0$  we have  $U \in \mathbb{R}^{n_2 \times n_2}$ ,  $V \in \mathbb{R}^{n_0 \times n_2}$  and  $\Lambda_T \in \mathbb{R}^{n_2 \times n_2}$  positive diagonal. We set the initial condition for  $R_2$  by first picking  $n_2$  orthogonal vectors in  $\mathbb{R}^{n_1}$  yielding an  $n_1 \times n_2$  matrix  $S$  with orthogonal columns, and writing  $R_2(0) = S \Lambda_R U^t$  with  $\Lambda_R$  diagonal and positive. This is a restricted initial condition

since for the most general initial condition, if we are free to choose  $S$ ,  $\Lambda_R$  would be upper triangular. Since  $W_1(0) = W_2(0) = 0$  and  $R_2(0)T = S\Lambda_R\Lambda_T V^t$  then we will always have  $W_1 = S\Lambda_1 V^t$  for some  $\Lambda_1 \in \mathbb{R}^{n_2 \times n_2}$  diagonal, and  $W_2 = U\Lambda_2 S^t$  for some  $\Lambda_2 \in \mathbb{R}^{n_2 \times n_2}$  diagonal. This setup yields:

$$W_2 W_1 = U\Lambda_2 \Lambda_1 V^t, \quad (T - W_2 W_1) = U(\Lambda - \Lambda_2 \Lambda_1) V^t.$$

So that the matrix equations in (12) decouple into  $n_2$  pairs of scalar ODE's one for each of the  $n_2$  columns of  $V$ .

$$\begin{aligned} \dot{\Lambda}_2 &= (\Lambda_T - \Lambda_2 \Lambda_1) \Lambda_1 \\ \dot{\Lambda}_1 &= (\Lambda_R + \epsilon \Lambda_2) (\Lambda_T - \Lambda_2 \Lambda_1). \end{aligned} \tag{13}$$

We analyze one such pair of scalar equations:

$$\begin{aligned} \dot{\lambda}_2 &= (\lambda_T - \lambda_2 \lambda_1) \lambda_1 \\ \dot{\lambda}_1 &= (\lambda_R + \epsilon \lambda_2) (\lambda_T - \lambda_2 \lambda_1), \end{aligned} \tag{14}$$

assuming without loss of generality that  $0 < \lambda_T \leq 1$  and  $\lambda_R \ll \lambda_T$ .

**Theorem 1.** *Define  $e = \lambda_T - \lambda_2 \lambda_1$ , and assume  $\lambda_1(0) = 0, \lambda_2(0) = 0$ . Then  $e^2$  converges exponentially fast to 0 and the rate of convergence increases as  $\epsilon$  increases.*

### 3.2 Deeper networks

For deeper networks we have the following equations for URFB:

$$\begin{aligned} \dot{W}_k &= e W_1^t \cdots W_{k-1}^t \\ &\vdots \\ \dot{W}_i &= (R_{i+1}(0) + \epsilon W_{i+1}^t) \cdots (R_k(0) + \epsilon W_k^t) e W_1^t \cdots W_{i-1}^t \\ &\vdots \\ \dot{W}_1 &= (R_2(0) + \epsilon W_2^t) \cdots (R_k(0) + \epsilon W_k^t) e, \end{aligned} \tag{15}$$

where  $e = T - W_k \cdots W_1$ ,  $T \in \mathbb{R}^{n_k \times n_0}$  and  $W_i \in \mathbb{R}^{n_i \times n_{i-1}}, i = 1, \dots, k$ .

Now let  $T = U \Lambda_T V^t$  be the SVD of  $T$ . Assuming  $n_k \leq n_0, n_1, \dots, n_{k-1}$  we have  $U \in \mathbb{R}^{n_k \times n_k}, V \in \mathbb{R}^{n_0 \times n_k}$  and  $\Lambda_T \in \mathbb{R}^{n_k \times n_k}$  positive diagonal. We set the initial condition for  $R_k$  by first picking  $n_k$  orthogonal vectors in  $\mathbb{R}^{n_{k-1}}$  yielding an  $n_{k-1} \times n_k$  matrix  $U_k$  and then writing  $R_k(0) = U_k \Lambda_{R,k} U_k^t$  with  $\Lambda_{R,k} \in \mathbb{R}^{n_k \times n_k}$  diagonal and positive and  $U_k \in \mathbb{R}^{n_{k-1} \times n_k}$  with orthogonal columns. For general  $i$  choose  $U_i \in \mathbb{R}^{n_{i-1} \times n_k}$  orthogonal,  $\Lambda_{R,i} \in \mathbb{R}^{n_k \times n_k}$  positive and diagonal, and set  $R_i(0) = U_i \Lambda_{R,i} U_i^t$ . Write  $W_i = U_{i+1} \Lambda_i U_i^t, i = 1, \dots, k$  and with  $U_{k+1} = U$ , and assume  $\Lambda_i(0) = 0$  then the system (15) decouples into  $n_k$  scalar equations one for each of the directions in  $U, V$ :

$$\begin{aligned} \dot{\lambda}_k &= e \lambda_{k-1} \cdot \lambda_1 \\ &\vdots \\ \dot{\lambda}_i &= (\lambda_{R,k} + \epsilon \lambda_k) \cdots (\lambda_{R,i+1} + \epsilon \lambda_{i+1}) e \lambda_{i-1} \cdots \lambda_1 \\ &\vdots \\ \dot{\lambda}_1 &= (\lambda_{R,k} + \epsilon \lambda_k) \cdots (\lambda_{R,2} + \epsilon \lambda_2) e, \end{aligned} \tag{16}$$

with  $\lambda_i(0) = 0$  and  $\lambda_{R,i} > 0$  random. This implies that  $\lambda_i$  are increasing and  $e$  is always positive. Multiplying the  $i$ 'th equation by  $(\lambda_{R,i} + \epsilon \lambda_i)$  and the  $i-1$ 'th equation by  $\lambda_{i-1}$  we get the equality

$$\dot{\lambda}_i (\lambda_{R,i} + \epsilon \lambda_i) = \dot{\lambda}_{i-1} \lambda_{i-1}, i = 2, \dots, k.$$

Since  $\lambda_i(0) = 0$  we can integrate and get

$$\lambda_{R,i} \lambda_i + \frac{\epsilon}{2} \lambda_i^2 = \frac{1}{2} \lambda_{i-1}^2 \tag{17}$$

Rewriting  $e = \lambda_T - \prod_{i=1}^k \lambda_i$ , we have

$$\begin{aligned} \frac{\dot{e}^2}{2} &= -e \sum_{i=1}^k \dot{\lambda}_i \prod_{j \neq i} \lambda_j = -e^2 \sum_{i=1}^k \prod_{j=1}^{i-1} \lambda_j^2 \prod_{j=i+1}^k \lambda_j (\lambda_{R,j} + \epsilon \lambda_j) \\ &= -e^2 \sum_{i=1}^k \prod_{j=1}^{i-1} \lambda_j^2 \prod_{j=i+1}^k \left( \frac{\epsilon}{2} \lambda_j^2 + \frac{1}{2} \lambda_{j-1}^2 \right) \end{aligned} \tag{18}$$

where the third equality follows from (17). It follows that for each  $\epsilon$  the error converges

exponentially fast to 0 and if it can be shown that  $\lambda_i$  are increasing in  $\epsilon$  the convergence rate is increasing with  $\epsilon$ . We are able to show this for  $k = 3$ .

**Theorem 2.** *For  $k = 3$ , assume  $\lambda_1(0) = 0, \lambda_2(0) = 0$ . Assume  $\lambda_{R,2}, \lambda_{R,3} < \delta \ll \lambda_T < 1$ , and assume  $\lambda_{R,2} > \frac{1+\sqrt{1+\epsilon}}{2}\lambda_{R,3}$ , then  $\lambda_1, \lambda_2$  and  $\lambda_3$  are increasing in  $\epsilon$  so that  $e$  converges faster to 0 as  $\epsilon$  increases.*

### 3.3 Simulation

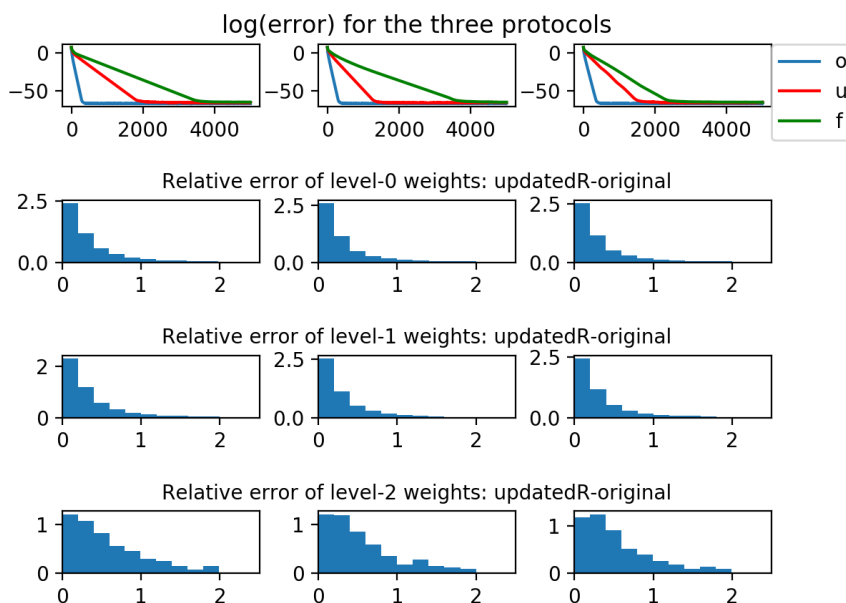


Figure 3: Top: comparison of log-error rates as a function of iteration for original SGD - 'o', FRFB - 'f', URFB - 'u'. Results for three runs of the experiment. Last three rows, for each level of the network a comparison of the relative difference of the URFB weights with SGD weights.

As a reality check for the theoretical results we simulated the following setting. An input layer of dimension 40, two intermediate layers of dimension 100 and an output layer of dimension 10.  $W_1 \in R^{40 \times 100}, W_2 \in R^{100 \times 100}, W_3 \in R^{100 \times 10}$ . We set  $T = W_1 W_2 W_3 \in R^{40 \times 10}$ . We then initialize the three matrices randomly as  $W_i(0), i = 1, 2, 3$ . With the same

initialization we then run equation (15) with  $R_i(0) = W_i(0)^t, \epsilon = 1$ , which corresponds to regular back-propagation,  $R_i$  - random,  $\epsilon = 1$ , which correspond to URFB, and  $R_i$  -random,  $\epsilon = 0$ , which corresponds to FRFB. We run 5000 iterations until all 3 algorithms have negligible error. We see the results in figure 3. In the first row, for 3 different runs we show the log-error as a function of iteration, and clearly URFB converges faster than FRFB. Since the initial values of  $W_i$  are the same in all three methods, in each run we can safely compare the weights coordinate by coordinate at the end of the iteration - we don't expect the weights get permuted. We show the relative error in the weights between SGD and URFB for the three layers and for the three runs. Despite the fact that the error is effectively zero, the resulting weights are not the same, namely the initial conditions are not forgotten with time.

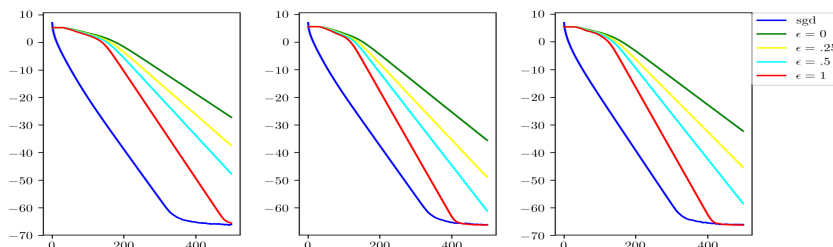


Figure 4: A comparison of log-error curves as a function of iteration at different levels of  $\epsilon = 0, .25, .5, 1.$ , alongside the log error curve for SGD. We show three different runs of the experiment.

In another experiment for FRFB,  $\epsilon = 0$  and *URFB*,  $\epsilon = .25, .5, 1.$ , we initialize all the feedforward weights at 0. The feedback weights are initialized randomly, and the same initialization is used for all values of  $\epsilon$ . Figure 4 clearly demonstrates the increase in the convergence rate of the error as  $\epsilon$  increases.

## 4 Experiments

We report a number of experiments comparing the updated (URFB) to the fixed feedback matrix (FRFB) and comparing the multi-class hinge loss function to the cross-entropy with softmax loss. We first experiment with a very simple network with the following architecture:

`simpnet: conv 32 5x5;maxpool 3;drop .8; full conn. 500;drop .3;output`

We use the saturated non-linearity and the hinge loss function as given in (3), all conv layers are padded to maintain the same dimensions and maxpool layers are padded and use stride 2 to obtain exactly half the current dimension. The update is a simple SGD with a fixed time step of .1, and the network is trained for 1000 epochs with batch-size of 500. We make a point to avoid any adaptive normalization layers as these require a complex gradient that is not amenable to simple neural computations. We avoid the more sophisticated time step adaptations which depend on previous updates and some normalizations, which again do not seem amenable to simple neural computations. We also experiment with pruning the forward and backward connections randomly by 50%. In other words half of these connections are randomly set to 0. The results for CIFAR10 and CIFAR100 datasets are shown in table 1. We show the results of backpropagation (BP)  $R = W$  with softmax in the first row and note that the use of the unnormalized multi-class hinge loss - in the second row - leads to only a small loss in accuracy. All experiments with random feedback are performed with the hinge loss. For CIFAR10 the difference between R fixed - FRFB - and R updated - URFB - is small, but becomes more significant when connectivity is reduced to 50% and with the CIFAR100 database.

CIFAR10			CIFAR100		
	Train error (tied/untied)	Test error (tied/untied)		Train error	Test error
BP Softmax	.02	.25	BP Softmax	.05	.57
BP Hinge	.11	.27	BP Hinge	.19	.57
URFB	.07/.04	.31/.33	URFB	.20	.61
FRFB	.27/.30	.36/.37	URFB 50%	.45	.62
URFB 50%	.14/.06	.31/.36	FRFB	.54	.68
FRFB 50%	.38	.45	FRFB 50%	.73	.76

Table 1: Error rates for simple network with different update regimes and different losses. If no loss specified we used the hinge loss. URFB - Updated random feedback and, FRFB - Fixed random feedback. 50% refers to random connectivity.

Note that in the simple network the only layer propagating back an error signal is the fully connected layer. The first layer, which is convolutional, does not need to back-propagate an error.

We experiment with a deep network with multiple convolutional layers, and observe an even larger difference between R fixed and R updated. With the deep network FRFB performs very poorly. The deep architecture is given here.

`deepnet: conv 32 5x5;maxpool 3; conv 32 3x3;conv 32 3x3; maxpool 3;drop .8;  
conv 32 3x3;conv 32 3x3; maxpool 3;drop .3; full conn. 500; output`

Finally we try an even deeper network with residual layers as in [3]. This means that after every pair of consecutive convolutional layers at the same resolution we introduce a layer that adds the two previous layers with no trainable parameters. This architecture was found to yield improved results with less layers on a variety of datasets.



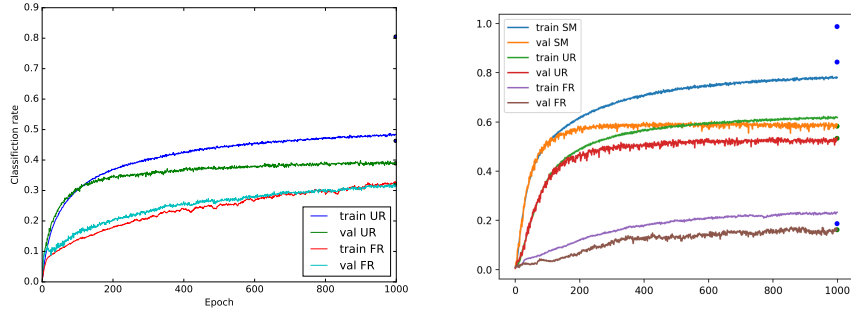


Figure 5: Evolution of error rates for simple and deeper network as function of epochs.

CIFAR100 - deep			CIFAR100 - deeper		
	Train error	Test error		Train error	Test error
BP Softmax	.18	.5	BP Softmax	.01	.42
BP Hinge	.38	.51	BP Hinge	.06	.42
URFB	.29	.52	URFB	.16	.47
URFB 50%	.41	.58	URFB 50%	.23	.56
FRFB	.79	.81	FRFB	.81	.84
FRFB 50%	.79	.89	FRFB 50%	.96	.96

Table 2: Error rates for the **deepnet** and **deepernet** .

**deepernet**: conv 16 3x3; conv 16 3x3; SUM; conv 32 3x3; conv 32 3x3; SUM; maxpool 3; drop .5;  
conv 64 3x3; conv 64 3x3; SUM; maxpool 3;  
conv 128 3x3; conv 128 3x3; SUM; maxpool 3; drop .8;  
full conn. 500; output

We see that for the default BP with softmax or hinge loss the error rate decreases from 50% with **deepnet** to 42% with **deepernet**. URFB also shows a decrease in error between **deepnet** and **deepernet** and again FRFB performs very poorly.

#### 4.1 Untying the convolutional layers

We also experiment with ‘untied’ sparse connectivities determined by the corresponding convolutional layer. Specifically we run the network for one epoch and a small time step of .01 with convolutional layers to mimic some form of spatial homogeneity that is predetermined. Then, some or all of the convolutional layers are changed into sparse fully connected layers, with connectivity determined by the matrix associated to the convolution. Subsequently all non-zero terms in the matrix are updated independently, as opposed to the convolutional update that ties all weights corresponding to the same feature and displacement across all locations. This is implemented using tensorflow sparse tensor operations. This is significantly slower and requires more memory than

the ordinary convolutional layers. The error rates are very similar to those with the original convolutional layers even with the deeper networks. In table 1, for CIFAR10, we show a comparison of error rates of each training protocol with a convolutional layer to that with a corresponding sparse fully connected layer. Despite the fact that the weights are updated without being tied across space, the final connectivity matrix retains a strong spatial homogeneity. In other words at each location of the output layer one can restructure the weights to a filter and inspect how similar these filters are across locations. We presume that this is due to the fact that in the data local structures are consistent across space. In figure 6 we show a couple of these 5x5 filters across four different locations in the 32x32 grid in the trained *simpnet*. We see that even after 1000 iterations there is significant similarity in the structure of the filters despite the fact that they were updated independently for each location.

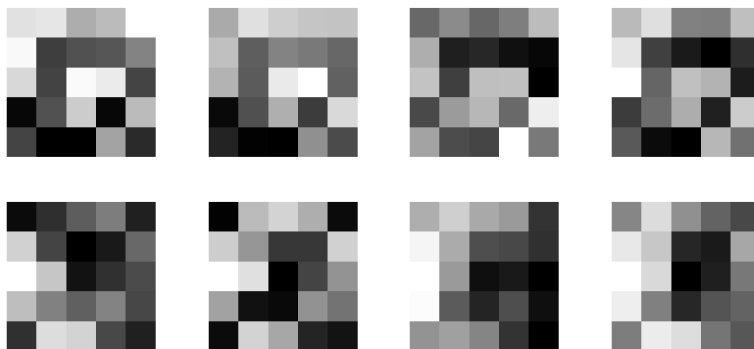


Figure 6: Corresponding filters extracted from the sparse connectivity matrix at 4 different locations on the 32x32 grid.

We also experiment with a deeper network:

```
deepernet_s: conv 16 3x3; conv 16 3x3; SUM; maxpool 3, stride 3; drop .5;
             conv 64 3x3; conv 64 3x3; SUM; maxpool 2, stride 2;
             conv 64 2x2; conv 64 2x2; SUM; maxpool 2, stride 2; drop .5;
             full conn. 500; output
```

Here we could not run all convolutional layers as fully connected sparse layers due to memory constraints on our GPUs. Instead we ran the network for 100 epochs with the regular convolutional layers, then we froze the first layer and retrained the remaining layers from scratch using the untied architecture, see table 3. This would mimic a situation where the first convolutional layer perhaps corresponding to V1 has connections that are predetermined and not subject to synaptic

modifications. Once more, we see that the untied layers with URFB reach error rates similar to those of the regular convolutional layers with standard gradient descent. And again, we observe that with a deeper network FRFB performance is much worse.

CIFAR10		
	Train error (tied/untied)	Test error (tied/untied)
BP Softmax	.21	.21
BP Hinge	.22	.22
URFB	.21/.06	.23/.29
FRFB	.51/.53	.56/.75

Table 3: Experiments with untying the convolutional layers on a deeper architecture. The dashes represent the fact that validation set error rates start increasing after a certain point.

## 5 Discussion

We have added some features to the original idea proposed in [7] that yield a more biologically plausible version of back propagation with error rates comparable to the standard BP algorithm. Specifically we have introduced a cost function whose derivatives lead to local Hebbian updates with a proposal for how the associated error signal could be implemented in a network, and we have added a Hebbian update of the feedback weights. We have shown theoretically, in the linear setting that adding the update to the feedback weights accelerates the convergence of the error to zero.

These contributions notwithstanding, there are still many aspects of this learning algorithm that are far from biologically plausible. One important issue is the timing of the feedforward and feedback weight updates that needs to be very tightly controlled. The update of the feedforward and feedback connections between layer  $l$  and  $l + 1$  requires the error signal to layer  $l + 1$  to have replaced the the feedforward signal in all its units, while the feedforward signal is maintained in layer  $l$ . An important component of the model proposed in [9] are the synaptic tags that maintain the information on the firing of the pre and post-synaptic neurons allowing for a later synaptic modification based on some reinforcement signal. An alternative direction of research would be to investigate the possibility of desynchronizing the updates, i.e. making the learning process more stochastic. If images of similar classes are shown in sequence it could be that it is not so important when the update occurs, as long as the statistics of the error signal and the feedforward signal are the same. Another issue is that of the training protocol. We assume randomly ordered presentation of data from all the classes, many hundreds of times. A more natural protocol would be to learn classes one at a time, perhaps occasionally refreshing the memory of previously learned ones. Because our loss function is local and updates to each class label are independent, one could potentially experiment with alternative protocols and see if they are able to yield similar error rates.

## 6 Proofs

*Proof of Theorem 1.* For  $k = 2$  equation (18) reduces to

$$\dot{e}^2 = -2e^2(\lambda_1^2 + \frac{1}{2}\lambda_1^2 + \frac{\epsilon}{2}\lambda_2^2). \quad (19)$$

Since  $\lambda_T, \lambda_R > 0$  and  $\lambda_1(0) = \lambda_2(0) = 0$  we see that  $\lambda_1$  and  $\lambda_2$  are increasing in time, and so after a finite time are uniformly bounded away from 0. This implies that the error goes to 0 exponentially fast. We also note that  $\lambda_1\lambda_2 = \lambda_T$  is a stationary point, so that  $\lambda_1\lambda_2 \leq \lambda_T$  always holds. If we can show that the factor of  $-e^2$  increases with  $\epsilon$  then the rate of convergence of  $e$  to zero increases with  $\epsilon$ .

Solving for  $\lambda_i$  in equation (17) and taking the positive solution we can write

$$\begin{aligned} \lambda_i &= G(\lambda_{i-1}, \lambda_{R,i}, \epsilon) \\ \lambda_{i-1} &= H(\lambda_i, \lambda_{R,i}, \epsilon), \end{aligned} \quad (20)$$

where

$$\begin{aligned} F(x, \lambda_R, \epsilon) &= \sqrt{\lambda_R^2 + \epsilon x^2}, \\ G(x, \lambda_R, \epsilon) &= \frac{F(x, \lambda_R, \epsilon) - \lambda_R}{\epsilon} = \frac{x^2}{F(x, \lambda_R, \epsilon) + \lambda_R}, \text{ and} \\ H(x, \lambda_R, \epsilon) &= \sqrt{2\lambda_R x + \epsilon x^2}. \end{aligned} \quad (21)$$

If we show that  $\lambda_1$  increases with  $\epsilon$ , then, by (20),  $\sqrt{\epsilon}\lambda_2 = \sqrt{\lambda_R^2/\epsilon + \lambda_1^2} - \lambda_R/\sqrt{\epsilon}$ , is easily seen to increase with  $\epsilon$  since  $\lambda_1$  and  $\lambda_R$  are positive. (In general, for any positive function  $g(\epsilon)$  that is increasing in  $\epsilon$  the function  $f(\epsilon) = \sqrt{c^2/\epsilon + g(\epsilon)} - c/\sqrt{\epsilon}$  is increasing w.r.t to  $\epsilon$ .) Thus  $\epsilon\lambda_2^2$  is increasing in  $\epsilon$  and the factor of  $-e^2$  in equation (19) is increasing in  $\epsilon$ .

Since  $\lambda_2 = G(\lambda_1, \lambda_R, \epsilon)$  we get the scalar equation for  $\lambda_1$  as

$$\dot{\lambda}_1 = F(\lambda_1, \lambda_R, \epsilon)(\lambda_T - G(\lambda_1, \lambda_R, \epsilon)\lambda_1) \equiv f_1(\lambda_1, \epsilon) \quad (22)$$

Let  $h > 0$  be a small increment and write,

$$\dot{\lambda}_\epsilon = f(\lambda_\epsilon, \epsilon), \quad \dot{\lambda}_{\epsilon+h} = f(\lambda_{\epsilon+h}, \epsilon + h).$$

Denote  $\Delta = \lambda_{\epsilon+h} - \lambda_\epsilon$  then to first order

$$\dot{\Delta} = \frac{\partial f}{\partial \lambda}(\lambda_\epsilon, \epsilon)\Delta + \frac{\partial f}{\partial \epsilon}(\lambda_\epsilon, \epsilon).$$

So if the second term is positive and the initial condition  $\Delta(0) = 0$  then, using the formula for the solution to first order ODE's,  $\Delta$  is always positive, so that  $\lambda_\epsilon$  is increasing in  $\epsilon$ . In our setting since

$$\frac{\partial F(x, \lambda_R, \epsilon)}{\partial \epsilon} = \frac{x^2}{2F(x, \lambda_R, \epsilon)} > 0, \quad (23)$$

$$\frac{\partial G(x, \lambda_R, \epsilon)}{\partial \epsilon} = -\frac{x^4}{2(F(x, \lambda_R, \epsilon) + \lambda_R)^2 F(x, \lambda_R, \epsilon)} < 0, \quad (24)$$

Consequently:

$$\frac{\partial f_1}{\partial \epsilon} = \frac{e\lambda_1^2}{2F(\lambda_1, \lambda_R, \epsilon)} + F\lambda_1 \frac{\lambda_1^4}{2(F(\lambda_1, \lambda_R, \epsilon) + \lambda_R)^2 F(\lambda_1, \lambda_R, \epsilon)} > 0. \quad (25)$$

Thus  $\lambda_1$  is increasing in  $\epsilon$ . □

*Proof of Theorem 2.* With  $k = 3$  (18) reduces to

$$\frac{\dot{e}^2}{2} = -e^2 \left[ \left( \frac{\epsilon}{2}\lambda_2^2 + \frac{3}{2}\lambda_1^2 \right) \cdot \left( \frac{\epsilon}{2}\lambda_3^2 + \frac{1}{2}\lambda_2^2 \right) + \lambda_1^2 \lambda_2^2 \right]. \quad (26)$$

We need to show that  $\lambda_1$  and  $\lambda_2$  are increasing in  $\epsilon$ . The term  $\epsilon\lambda_3^2$  can be handled just like the term  $\epsilon\lambda_2^2$  in the case  $k = 2$ .

Write  $H(\lambda_2) = H(\lambda_2, \lambda_{R,2}, \epsilon)$ ,  $F(\lambda_2) = F(\lambda_2, \lambda_{R,3}, \epsilon)$ ,  $G(\lambda_2) = G(\lambda_2, \lambda_{R,3}, \epsilon)$  functions of  $\lambda_2$ . Furthermore set

$$\begin{aligned} G_2(\lambda_1) &= G(\lambda_1, \lambda_{R,2}, \epsilon), \\ G_3(\lambda_1) &= G(G_2(\lambda_1), \lambda_{R,3}, \epsilon), \\ F_2(\lambda_1) &= F(\lambda_1, \lambda_{R,2}, \epsilon), \\ F_3(\lambda_1) &= F(G_2(\lambda_1), \lambda_{R,3}, \epsilon) \end{aligned}$$

all functions of  $\lambda_1$ . Write the equations for  $\lambda_1, \lambda_2$  with all other variables eliminated:

$$\begin{aligned} \dot{\lambda}_2 &= F(\lambda_2) (\lambda_T - G(\lambda_2)\lambda_2 H(\lambda_2)) H(\lambda_2) \\ \dot{\lambda}_1 &= F_3(\lambda_1) F_2(\lambda_1) (\lambda_T - G_3(\lambda_1) G_2(\lambda_1) \lambda_1) \end{aligned} \quad (27)$$

We have

$$\frac{dF_2}{d\epsilon} = \frac{\lambda_1^2}{2F_2} \quad (28)$$

$$\frac{dG_2}{d\epsilon} = \frac{-\lambda_1^4}{2(F_2 + \lambda_{R,2})^2 F_2} \quad (29)$$

$$\frac{dF_3}{d\epsilon} = \frac{\partial F_3}{\partial G_2} \frac{\partial G_2}{\partial \epsilon} + \frac{\partial F_3}{\partial \epsilon} = \frac{G_2^2}{2F_3} - \frac{\epsilon G_2}{F_3} \frac{dG_2}{d\epsilon} \quad (30)$$

$$\frac{dG_3}{d\epsilon} = -\frac{G_2^4}{2(F_3 + \lambda_{R,3})^2 F_3} - \frac{\epsilon G_2}{F_3} \frac{\lambda_1^4}{2(F_2 + \lambda_{R,2})^2 F_2} \quad (31)$$

$$\frac{dH}{d\epsilon} = \frac{\lambda_2^2}{2H} \quad (32)$$

For  $\lambda_1$  the derivative of the right hand side of (27) with respect to  $\epsilon$  is

$$\frac{dF_3}{d\epsilon} F_2 e + F_3 \frac{dF_2}{d\epsilon} e - F_3 F_2 \left[ \frac{dG_3}{d\epsilon} G_2 \lambda_1 + G_3 \frac{dG_2}{d\epsilon} \lambda_1 \right].$$

Since  $F_2, G_2, F_3, G_3 > 0$  and the derivatives of  $G_2, G_3$  with respect to  $\epsilon$  are negative the second and third terms are positive. It is left to show that  $\frac{dF_3}{d\epsilon} > 0$ . Substituting  $G_2 = \frac{\lambda_1^4}{(F_2 + \lambda_{R,2})^2}$  in the first term we have:

$$\frac{G_2^2}{2F_3} - \frac{\epsilon G_2}{F_3} \frac{dG_2}{d\epsilon} = \frac{\lambda_1^4}{2F_3(F_2 + \lambda_{R,2})^2} \left[ 1 - \frac{\epsilon G_2}{F_2} \right] = \frac{\lambda_1^4}{2F_3(F_2 + \lambda_{R,2})^2} \frac{\lambda_{R,2}}{F_2} > 0.$$

For  $\lambda_2$  the derivative of the right hand side of (27) with respect to  $\epsilon$ :

$$\frac{\lambda_2^2}{2F} eH + F \left[ \frac{\lambda_2^4}{2(F + \lambda_{R,3})^2 F} \lambda_2 H - G \frac{\lambda_2^2}{2H} \lambda_2 \right] H + F e \frac{\lambda_2^2}{2H} = T_1 + T_2 + T_3.$$

The first and third terms are positive. For the second term we have substituting  $G = \frac{\lambda_2^2}{F + \lambda_{R,3}}$ ,

$$\begin{aligned} T_2 &= \left[ \frac{\lambda_2^4}{2(F + \lambda_{R,3})^2 F} \lambda_2 H - G \frac{\lambda_2^2}{2H} \lambda_2 \right] = \frac{\lambda_2^5}{2} \left[ \frac{H}{(F + \lambda_{R,3})^2 F} - \frac{1}{H(F + \lambda_{R,3})} \right] \\ &= \frac{\lambda_2^5}{(F + \lambda_{R,3})^2 F H} [H^2 - (F + \lambda_{R,3})F]. \end{aligned}$$

The last factor is

$$2\lambda_{R,2}\lambda_2 - \lambda_{R,3}^2 - \lambda_{R,3}\sqrt{\lambda_{R,3}^2 + \epsilon\lambda_2^2}. \quad (33)$$

Assume for small  $\delta < 1$  that  $\lambda_{R,2}, \lambda_{R,3} < \delta < \lambda_T$  then an order computation shows that as long as  $\lambda_2 \leq \delta$  then  $T_1 + T_3 = o(\delta^2)$  whereas  $0 > T_2 = o(\delta^5)$  and so the sum is positive. When  $\lambda_2 > \lambda_{R,2}, \lambda_{R,3}$ , then the expression in (33) is bounded below by  $2\lambda_{R,2}\lambda_2 - \lambda_{R,3}\lambda_2 - \lambda_{R,3}\sqrt{1 + \epsilon}\lambda_2 > 0$

if  $\lambda_{R,2} > \frac{1+\sqrt{1+\epsilon}}{2}\lambda_{R,3}$ . Thus  $T_2 > 0$ . In summary both  $\lambda_1, \lambda_2$  are increasing in  $\epsilon$  as long as  $\lambda_{R,2}, \lambda_{R,3} < \delta < \lambda_T$ .  $\square$

## References

- [1] Y. Amit and M. Mascaró. An integrated network for invariant visual detection and recognition. *Vision Research*, 43:2073–2088, 2003.
- [2] Yali Amit and Jacob Walker. Recurrent network of perceptrons with three state synapses achieves competitive classification on real inputs. *Frontiers in Computational Neuroscience*, 6:39, 2012.
- [3] H Kaiming, Z. Xiangyu, R. Shaoqing, and S. Jian. Deep residual learning for image recognition. *2016 IEEE Conference on Computer Vision and Pattern Recognition (CVPR)*, pages 770–778, 2016.
- [4] Nikolaus Kriegeskorte. Deep neural networks: A new framework for modeling biological vision and brain information processing. *Annual Review of Vision Science*, 1(1):417–446, 2015.
- [5] G. La Camera, A. Rauch, H. R. Luscher, W. Senn, and S. Fusi. Minimal models of adapted neuronal response to in vivo-like input currents. *Neural Comput*, 16:2101–24, 2004.
- [6] Qianli Liao, Joel Z. Leibo, and Tomaso Poggio. How important is weight symmetry in back-propagation? In *Proceedings of the Thirtieth AAAI Conference on Artificial Intelligence*, AAAI’16, pages 1837–1844. AAAI Press, 2016.
- [7] Timothy P. Lillicrap, Daniel Couden, Douglas B. Tweed, and Colin J. Akerman. Random synaptic feedback weights support error backpropagation for deep learning. *Nature Communications*, 7:13276 EP –, 11 2016.
- [8] Adam H. Marblestone, Greg Wayne, and Konrad P. Kording. Toward an integration of deep learning and neuroscience. *Frontiers in Computational Neuroscience*, 10:94, 2016.
- [9] Pieter R. Roelfsema and Anthony Holtmaat. Control of synaptic plasticity in deep cortical networks. *Nature Reviews Neuroscience*, 19:166 EP –, 02 2018.
- [10] Andrew M. Saxe, James L. McClelland, and Surya Ganguli. Exact solutions to the nonlinear dynamics of learning in deep linear neural networks. *CoRR*, abs/1312.6120, 2013.
- [11] Shai Shalev-Shwartz, Yoram Singer, Nathan Srebro, and Andrew Cotter. Pegasos: Primal estimated sub-gradient solver for svm. *Math. Program*, 127:3–30, 03 2011.